

## Barkhausen statistics from a single domain wall in thin films studied with ballistic Hall magnetometry

D. A. Christian,\* K. S. Novoselov, and A. K. Geim

*Department of Physics and Astronomy, University of Manchester, Oxford Road, Manchester M13 9PL, United Kingdom*

(Received 11 October 2005; revised manuscript received 16 February 2006; published 3 August 2006)

The movement of a micron-size section of an individual domain wall in a uniaxial garnet film was studied using ballistic Hall micromagnetometry. The wall propagated in characteristic Barkhausen jumps, with the distribution in jump size  $S$ , following the power-law relation,  $D(S) \propto S^{-\tau}$ . In addition to reporting on the suitability of employing this alternative technique, we discuss the measurements taken of the scaling exponent  $\tau$ , for a single domain wall in a two-dimensional sample with magnetization perpendicular to the surface, and low pinning center concentration. This exponent was found to be  $1.14 \pm 0.05$  at both liquid helium and liquid nitrogen temperatures.

DOI: [10.1103/PhysRevB.74.064403](https://doi.org/10.1103/PhysRevB.74.064403)

PACS number(s): 75.60.Ej, 05.40.-a, 05.65.+b, 85.75.Nn

### I. INTRODUCTION

The Barkhausen effect is the name given to the nonreproducible and discrete propagation of magnetic domain walls due to an applied magnetic field. The walls remain immobile for inconstant lengths of time, before shifting to a new stable configuration in either a single jump, or a series of jumps (commonly referred to as an “avalanche”). It was discovered in 1919,<sup>1</sup> and has seen a renewed interest as a result of recent work, connecting it with various aspects of noise and critical phenomena.<sup>2–8</sup> An analysis of Barkhausen statistics has been proven as an effective nondestructive method of probing physical characteristics of a material, including the level of lattice disorder, and the tensile stress exerted upon a sample.

The effect is often quoted as an example of a system exhibiting self-organized criticality (SOC), an idea that reflects the fact that domain walls in a ferromagnetic material will exhibit Barkhausen noise without needing any specific tuning of conditions,<sup>2,3,5,6,9,10</sup> and that the size,  $S$ , and duration,  $T$ , of the avalanches have been found to show scaling behavior, and hence follow power laws. The power law for jump size can be expressed as

$$D(S) = S^{-\tau} f(S/S_0), \quad (1)$$

where  $S_0$  is the cutoff limit, and  $\tau$  is the scaling exponent, which is linearly dependent on the applied magnetic driving rate.

Most previous studies<sup>3,5–8,11–13</sup> have experimentally determined this exponent for bulk three-dimensional samples of a soft, ferromagnetic material, using a pickup coil to measure flux variations. This inductive method allows movement across a large system of domain walls to be detected, though it cannot differentiate between a single jump and a large number of jumps occurring in several places at once. However, comparatively little work has been done with two-dimensional samples, as a pickup coil receives a greatly decreased signal, making it difficult to resolve against background noise. Accordingly, although the inductive method has been employed in this area successfully by one group,<sup>14</sup> most experiments in this area have been based on different techniques, such as MOKE<sup>15,16</sup> and MFM.<sup>17</sup> With the exception of Ref. 17, the two-dimensional samples all

feature in-plane magnetization and thus have negligible demagnetization fields, which have been shown to significantly affect Barkhausen statistics.<sup>5</sup> The authors of Ref. 17 scanned the surface of a manganite film using magnetic force microscopy. This surface had a highly granular structure, which meant that the domain walls were being pinned on a large number of extended pinning regions, such as grain boundaries and dislocations. Again, this is likely to affect the way in which a wall is able to propagate, and so change the scaling exponents. These issues make it difficult to accurately relate such experimental results to the idealized theoretical models.

As an alternative to the previous methods used to study the Barkhausen effect, we describe here our use of ballistic Hall micromagnetometry. As a result of the convenient and sensitive detection of local magnetic flux that this technique offers, it has been used to study a wide range of other phenomena, including magnetization switching behavior in mesoscopic superconductors,<sup>18,19</sup> and in single and arrayed nanostructures,<sup>20,21</sup> the nucleation<sup>22</sup> and annihilation<sup>23</sup> of domains, and the coercivity of a single pinning center.<sup>24</sup> Although larger Hall probes operating in the diffusive regime have been used to study the Barkhausen effect previously, the focus of that research was qualitative observation of domain reversal within bulk Nd-Fe-B samples.<sup>25</sup>

Our technique is closely related to that using a standard Hall cross layout, but with conducting channels constructed on the  $\mu\text{m}$  scale with very high mobility and a low level of defects. The particular device we used, shown as an inset in Fig. 1, was constructed from a GaAs/InGaAs heterostructure, which had a 2DEG embedded 60 nm below the surface, with an electron density of  $3.4 \times 10^{12} \text{ cm}^{-2}$ . This was formed into five adjacent crosses using standard lithographic techniques, three with a channel width of  $1.5 \mu\text{m}$ , and the remaining two with channels of  $1.0 \mu\text{m}$ , which are standard sizes proven to work effectively for ballistic Hall micromagnetometry. The high mobility of the 2DEG means that transport along the conducting channels of the device is ballistic. Such Hall probes were found to be the most sensitive for our work.<sup>26</sup>

For one of our Hall crosses, when a ballistic current is travelling along one channel, the Hall resistance  $R_{xy}$ , is given by the equation

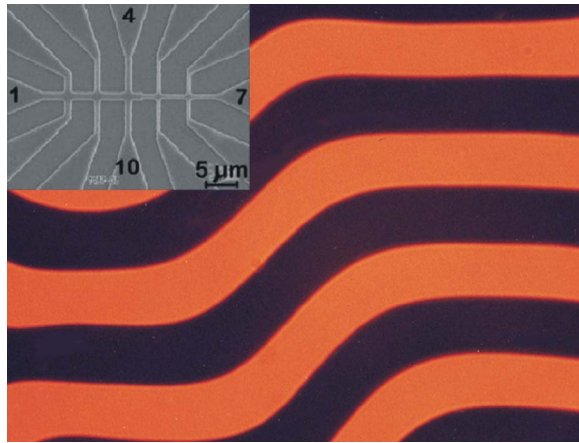


FIG. 1. (Color online) A micrograph of part of our garnet sample, visualized using transmitted polarized light. A SEM image of the Hall cross device used is shown to scale, as an inset. On the scale of a single Hall cross, it can be seen that an individual domain wall is close to being straight. The three adjacent Hall crosses to the left of the image have a square intersection area of  $2.25 \mu\text{m}^2$ , making the channels an order of magnitude smaller than the average width of a domain in the equilibrium state shown. The two crosses to the right have an area of  $1 \mu\text{m}^2$ . The connections to the device were numbered for easier reference, with a few of these labels shown. The results in this paper were taken using connections 1, 2, 7, and 12.

$$R_{xy} = \alpha_H \langle B \rangle R_H, \quad (2)$$

where  $\alpha_H$  is a coefficient relating to the geometrical design of the Hall cross (1.2 for our device),<sup>27</sup> and  $\langle B \rangle$  is the magnetic field averaged over the Hall cross intersection, shown as the shaded area in Fig. 2(a). The treatment of data is thus simplified as the precise field configuration across the intersection need not be determined, and gradual changes in the magnetic field can be measured accurately.<sup>28</sup> When a domain wall moves past this intersection or sensitive zone (SZ), the average magnetic field is altered, which induces a corresponding change in the Hall resistance, allowing an accurate measurement of the wall movement. The extended parts of the wall that are outside the SZ have a negligible effect on the Hall resistance.

We chose to employ this method in studying the Barkhausen effect exhibited by a single domain wall in a  $10 \mu\text{m}$  thick, ferromagnetic yttrium iron garnet (YIG) sample, as this can be considered, for the purposes of comparison with theory, to be very close to an ideal two-dimensional system, for reasons discussed later. At liquid helium temperatures, our samples have an exchange constant  $A = 1.8 \times 10^{-7} \text{ erg/cm}$ , and an anisotropy constant  $K = 1.4 \times 10^6 \text{ erg/cm}^3$ . The domain wall width  $\delta$ , is then given by  $\delta = \pi\sqrt{A/K} \approx 10 \text{ nm}$ . At higher temperatures,  $K$  decreases to  $4.7 \times 10^5 \text{ erg/cm}^3$ , and the wall therefore has an increased width of  $\approx 20 \text{ nm}$ .

These garnet samples display strong uniaxial anisotropy, so that the magnetization lies only in the two opposing directions perpendicular to the sample surface. This leads to a series of domains of alternating magnetization direction,

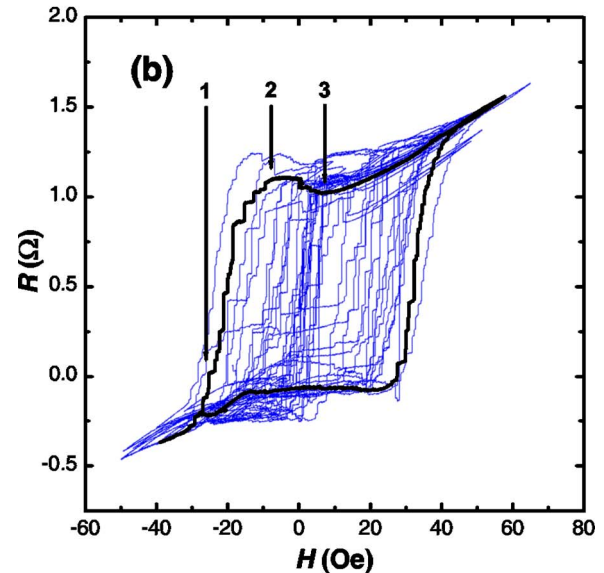
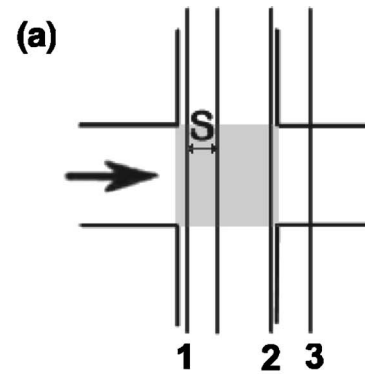


FIG. 2. (Color online) (a) A representation of several positions of a domain wall moving past the intersection or sensitive zone of a Hall cross, with this zone shown shaded. The large arrow represents the direction of motion of the wall. The size of jump  $S$ , as used in this paper, is defined as shown, for two arbitrary positions of the wall. (b) An example of data taken at 4.2 K, showing a typical set of 20 sweeps. The total change in magnetic field is quite small (just over 100 G), and so does not cause saturation. One loop has been highlighted to show more clearly the behavior of the domain wall and has numbered positions that correspond to the positions in (a).

which are separated by a system of  $180^\circ$  domain walls. An example of such a domain structure can be seen in Fig. 1, which shows a section of our garnet film pictured using transmitted polarized light, and displaying the tendency for the walls to form parallel to each other. In addition to producing this simple domain arrangement, the strong anisotropy prevents deformation of the domain wall away from the axis perpendicular to the sample surface.

This particular system of cylindrical domains is the usual result when the uniaxial anisotropy  $K_u \geq 2\pi M_s^2$ , which is true for our sample, and especially when the applied field is aligned with the easy axis of the specimen.<sup>30</sup> It has also been demonstrated that deviation from the easy axis is significantly lower in samples that, when arranged in parallel stripe domains of equal size, have a domain width approximately equal to the thickness of the sample. An examination of Fig.

1 reveals that the domain thickness is about  $10\ \mu\text{m}$ , which is equal to the garnet film thickness, indicating empirically that divergence of the walls from the easy axis is minimal.

Thus, the domain wall deforms only in the  $x$ - $y$  plane, while remaining straight in the  $z$  direction, i.e. parallel to the easy axis. It is this domain arrangement that categorizes the sample as two-dimensional, not in reference to the physical dimensions of the film, but to the reduced dimensionality of the domain walls themselves, which have lost a degree of freedom of distortion. The walls could alternatively be described as displaying one-dimensional vaulting, or bowing.<sup>29,31,32</sup>

A garnet film was also chosen, as it can be manufactured with a very low level of defects, and most of those present are pointlike pinning centers arising from imperfections in the surface (length scale  $\sim 10\ \text{nm}$ ),<sup>24</sup> and so the walls are straight over lengths of up to  $100\ \mu\text{m}$ . It can be seen from Fig. 1 that on the scale of a typical cross ( $\sim 1\ \mu\text{m}$ ), it is only a small section of a single domain wall that is being studied. At the temperatures used, this section is sufficiently small that it will remain straight. This assumption is supported by measurements taken at liquid helium temperature on two crosses simultaneously, when the crosses were aligned parallel to the domain wall.<sup>24</sup> In this instance identical movements were recorded by both crosses, meaning that walls move without bending over lengths of several  $\mu\text{m}$ . Therefore, the section of the domain wall under observation exhibits no bowing at all within the SZ, which means that at low temperatures the domain wall may effectively have even lower dimensionality.

One valuable consequence of the wall remaining straight while traversing the Hall cross is that the size of each jump can be expressed simply as a distance,  $S$ , as shown in Fig. 2(a). The maximum and minimum values of Hall resistance recorded over a full sweep correspond to the wall being at opposite sides of the cross, i.e., at positions 1 and 2 in Fig. 2(a). The average difference between these two resistance values is therefore equivalent to a domain wall movement equal in size to the branch width of the Hall cross used.

The combination of high anisotropy and low defects results in a system that is ideally suited for investigating the scaling exponents, especially at a low temperature, which is assumed in most models of the Barkhausen effect. The Barkhausen statistics will be characteristic of a domain wall system in a two-dimensional sample, with long-range dipolar interactions and with the demagnetizing field present as a result of the perpendicular magnetization.

## II. EXPERIMENTAL TECHNIQUE

The five Hall cross device is attached to the garnet sample, with a gap of under  $200\ \text{nm}$  between them.<sup>24</sup> The sample and device were placed at the center of a solenoid, so as to ensure a uniform applied field, and kept at either liquid nitrogen or liquid helium temperature. The field is perpendicular to the surface of the sample, and hence parallel to both possible magnetization directions. The ballistic current was directed down the long path of the Hall device (the horizontal path in Fig. 1), allowing the use of any of the five

crosses. We selected a cross with a channel width of  $1.5\ \mu\text{m}$  with which to take measurements, as it exhibited the lowest noise.

We used standard low-frequency lock-in techniques to measure the Hall resistance, culminating in several sets of data similar to the example in Fig. 2(b). From this raw data, we measured the size of each jump, allowing a histogram of the relative probabilities of each jump size to be plotted, which provided a value for  $\tau$ .

The section of the highlighted loop between positions 1 and 2 in Fig. 2(b) describes the normal movement of a domain wall across the SZ of the Hall cross by Barkhausen jumps. However, between positions 2 and 3, when the wall has passed fully across the SZ and begins to move away from the Hall cross, the jumps in the opposite direction to the trend are observed. This behavior is the result of the decay in the stray magnetic field as one moves away from a domain wall. Related to this external wall effect is the fact that the SZ does not have a uniform response over its area, with decreased sensitivity at the edges.

Recorded jumps arising from the edges and outside of the SZ are not related to the critical behavior of the Barkhausen effect and, if left mixed with the desired jump data, will distort the resultant jump size distribution. As a result, only the jumps that occur within the SZ, i.e., between positions 1 and 2, are included in the statistical analysis. The external wall effect has additional consequences, which are discussed in the next section.

We ensured that the wall under observation moved past the entire SZ for every sweep of the applied external field, so as to elicit consistent data, with a constant total variation in the Hall resistance for each loop. This was achieved by ramping the field at a constant rate so that the domain walls passed back and forth over the Hall probe, between positions either at or just outside the edge of the SZ, e.g., at positions 1 or 2 in Fig. 2. The direction of field sweep switched once the maximum response of the device had occurred, which was recognizable by the cessation of significant change in the Hall resistance.

The maximum allowed field was set at  $\pm 200\ \text{G}$  (approximately the saturation magnetization of our garnet film), although the field rarely reached this level, staying within the  $\pm 50\ \text{G}$  range. As the sample never reaches saturation, the simple wall propagation regime of magnetization is dominant, rather than those of domain nucleation or coalescence. These two processes, along with spontaneous spin rotation, are not governed by the same physical laws as the Barkhausen effect, and so the discussion in this paper is concerned with domain wall motion only.

## III. RESULTS AND DISCUSSION

The progress of the domain wall past the SZ is slow, such that a single sweep will take about an hour to complete. This has limited the number of recorded sweeps to 2792 at liquid nitrogen temperature, and 1429 at liquid helium temperature. In general, the jump distributions, plotted on double-log<sub>10</sub> scales, display the expected linear appearance for each temperature, with the gradients of the straight sections of the



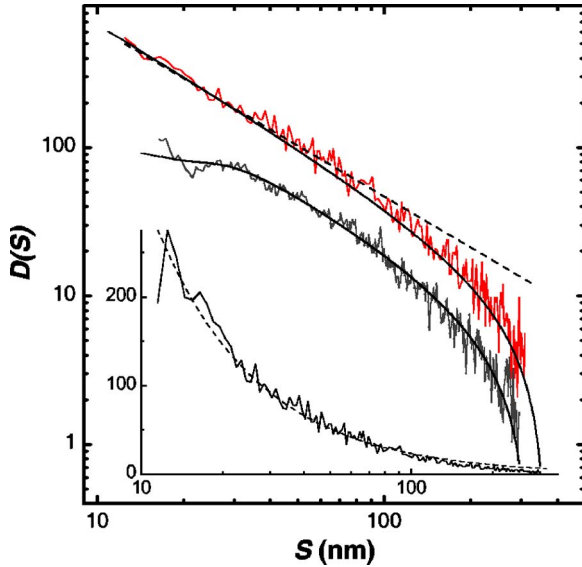


FIG. 3. (Color online) A comparison between the power-law behavior of a single domain wall at 77 K over 2792 sweeps (lower plot), and at 4.2 K over 1429 sweeps (upper plot). The frequency  $D(S)$  is a count of the number of occurrences of jumps of a given size, normalized per 1000 sweeps. The dashed line represents the best fit to both data, which gives a value of  $\tau$  of  $1.14 \pm 0.05$ . The solid, darker lines are fits with the same value of  $\tau$ , but taking into account behavior explained in the main text. The inset shows the data taken at 4.2 K with  $D(S)$  plotted on a linear scale. This demonstrates that the deviation at large jump sizes from the fitted line, also shown, is minimal.

lines giving the values for  $\tau$  [see Eq. (1)]. Figure 3 shows the data for both temperatures over a similar range of jump sizes. The number of occurrences of each value of  $S$  was normalized to give the frequency per 1000 sweeps,  $D(S)$ . The data at 4.2 K has been artificially moved up the  $D(S)$  scale by an arbitrary factor of 2 so as to prevent overlap, and allow easier viewing.

The chosen upper limit for displayed data was 300 nm, as there are few jumps occurring above this level, and consequently they are too scarce to be used to increase the accuracy of the gradient. The data are not shown for jump sizes smaller than  $\sim 10$  nm and  $\sim 15$  nm for 4.2 and 77 K, respectively, as below these levels it becomes very difficult to resolve jumps against the background noise. This does not represent the maximum resolution achievable with this technique, as a resolution of  $1 \text{ \AA}$  has already been reported.<sup>33</sup> However, this was achieved using Hall probes, which, although similar in design to the one described here, had a much lower electron concentration. The benefit of the higher concentration probes we have employed here is the ability to take measurements at room temperature, while the lower concentration probes must be used in liquid helium.

The dashed line in Fig. 3 is a logarithmic fit to the data of the form  $A/S^\tau$ , which on the log scales has a gradient of  $-1.14 \pm 0.05$  in the straight section of the data, for  $S$  below 120 nm. The error on the fitted gradient for the 4.2 K data was given by the fitting algorithm as  $\pm 0.024$ , but this is unrealistic considering the small range of the data. The quoted error represents the range of gradient values that have believ-

able agreement with this data. The 77 K data has a gradient of  $-1.14 \pm 0.048$ , though the range of data that strongly conforms to this is even less than for the helium temperature data. However, there is strong agreement between the data at the two temperatures for jump sizes greater than 30 nm, which implies that they are displaying identical statistical behavior. The agreement is even more obvious when the 4.2 K data is not shifted up the  $D(S)$  scale, as the normalized data for both temperatures overlap very closely.

Thus, the scaling exponent  $\tau$  has a constant value of 1.14 over the temperature range 4–77 K. The lack of a strong response to temperature variation has been observed previously in three-dimensional samples,<sup>34</sup> though thermally activated effects, such as domain wall creep, tend to become increasingly apparent in thin films as the temperature is increased.<sup>35</sup> Other previous research on thin film samples found the value of  $\tau$  to increase from 1.0 to 1.8 as the temperature was decreased from 300 to 10 K in an iron thin film.<sup>36</sup>

At jump sizes greater than  $\sim 120$  nm, there is a cutoff where the jump distributions deviate away from the fitted line. This deviation is accentuated due to the use of a logarithmic scale and the small numbers of recorded large jumps, as evidenced by Fig. 3 (inset), where the 4.2 K data are shown with  $D(S)$  plotted on a linear scale, and  $S$  on a logarithmic scale as before. From this plot it is apparent that the deviation is relatively small. The cutoff is present partly because of the insufficient size of the set of data used, but also due to the finite size effects caused by the physical size of the Hall cross employed. If the wall starts from a position inside the sensitive region, but in a single Barkhausen jump moves to a position outside or vice versa, then due to the external wall effect mentioned earlier, the measured size of the jump will be less than the true value. A typical sweep consists of about 25 to 30 jumps, two of which will exhibit this behavior, implying that 8% of jumps will have measured values lower than their true values. This will influence larger jump sizes both more often and with a greater effect than the smaller jumps. The absolute upper limit in recorded jump size is ultimately controlled by the size of the Hall junction. As ours was  $1.5 \text{ }\mu\text{m}$  across, this is the maximum value obtainable, though in practice this is unlikely to be observed.

Although the distributions for the two temperatures show a strong correlation for larger jumps, there is a noticeable dip in the 77 K data below  $S=30$  nm. One possible cause of this is the fact that real domain walls have finite width. As a result, two pinning centers which are positioned apart by a distance smaller than the domain wall width will affect the wall in the same way as a single, larger center. Once the wall is pinned at this location, jumps smaller than the distance required to escape from the center will not be observed. This would also cause a corresponding dip in the jump distribution at helium temperatures, which is not visible in the data shown. This is to be expected however, since at helium temperatures the width of a domain wall is reduced so the dip would only begin to manifest at the minimum displayed  $S$  value.

Using these ideas, we have derived an approximated equation of the form of Eq. (1), with the coefficient  $S_0$  replaced by the width of the Hall cross, that takes account of

the changed behavior at both extremes of  $S$ . Using this, fits made to the measured data at either temperature using  $\tau=1.14$  show a greatly increased correlation. These are the solid fitted lines shown with their associated datasets in Fig. 3.

Previous experimental work on 2D systems has produced different values, ranging from  $\tau$  being  $\sim 1.5$ ,<sup>14</sup> to  $\sim 1.1$ .<sup>15</sup> Our results are close to the lower of the two, although the authors offer no explanation as to the physical meaning of their value, so it is difficult to know whether the causes are the same in each case.

Using the basic ideas present in the CZDS model,<sup>5</sup> one might expect a value of  $\tau=1.33$  for a domain wall in a two-dimensional system [from the equation given where  $\tau=2-2/(d+1)$ , where  $d$  is the number of dimensions], and this has been used to support such measured values of  $\tau$ .<sup>16</sup> However, it has been suggested that this equation cannot be applied in such a straightforward way, as there are additional factors to consider with two-dimensional samples.<sup>32</sup> Among these is the high anisotropy that causes reduced domain wall roughness, as is evident for the walls in our sample, which are flat on the scale of the Hall probe. In such a case, renormalization group analysis has yielded a reduced value of  $\tau=1.25$ ,<sup>37</sup> though this is still larger than that observed in our experiment.

Another possible explanation for the small value of  $\tau$  is that a dimensional crossover as a result of small sample thickness has caused the Barkhausen statistics to correspond to a sample that has a dimensionality between integer values. This idea has been explored, based on a simulation of the Barkhausen effect.<sup>38</sup> The single-interface model used in this simulation predicts a crossover from  $\tau=1.275$  in bulk samples, to  $\tau=1.06$  in  $d=2$ , which would cover the value measured here. For a sample with dimensions and aspect ratio equal to those of our garnet film, the graphs given in the quoted paper predict a value of  $\tau=1.15$ , but again the effects of reducing the degrees of freedom of the domain wall are not explored.

The fact that  $\tau$  remains constant over the tested temperature range is unusual, as there are several ways in which a

decrease in thermal energy within the sample could be expected to change the statistics. First, this energy decrease would cause the wall to display less bowing, which would have the effect of reducing  $\tau$ . This effect will be small for our sample, partly because the bowing is already constrained by the anisotropy, and also because of the small size of the Hall cross intersection, so there is limited scope for constraining it further upon cooling below 77 K.

Alternatively, with lower thermal energy the wall will be more susceptible to becoming trapped by a pinning center during an avalanche, which will act to increase  $\tau$ , as the proportion of smaller jumps will increase. Films such as that which showed the marked change in  $\tau$ <sup>36</sup> will more noticeably demonstrate this effect than will our sample, as a result of the lack of out-of-plane magnetization allowing longer range interactions with the rest of the domain wall network.

The long-range interactions clearly play a major role in the way in which a domain wall is able to propagate through our material. The Hall cross used is so small that the domain wall can be approximated as being a one-dimensional object, traveling through the SZ of the cross without bending in any significant fashion. However, since this small section of wall is still coupled to the whole wall, and undergoing dipole interactions with other walls, we believe it produces the jump statistics expected for the whole wall network, i.e. the statistics from a wall able to bow or distort in one dimension.

Other models are usually based on the assumption that the dominant damping mechanism of domain wall motion is through the formation of eddy currents within the sample, which is not applicable to our samples, as they are nonconducting. One of the dominant forms of wall motion damping is through the interactions between the other domain walls via the demagnetization field. This field is not temperature dependent, and as it has a strong influence on Barkhausen statistics, this will tend to keep  $\tau$  constant.

#### ACKNOWLEDGMENTS

This work was supported by the EPSRC (UK). Many thanks to S. V. Dubonos for making the samples and devices that were used.

\*Electronic address: david@grendel.ph.man.ac.uk

<sup>1</sup>H. Barkhausen, *Phys. Z.* **20**, 401 (1919).

<sup>2</sup>P. J. Cote and L. V. Meisel, *Phys. Rev. Lett.* **67**, 1334 (1991).

<sup>3</sup>J. S. Urbach, R. C. Madison, and J. T. Markert, *Phys. Rev. Lett.* **75**, 276 (1995).

<sup>4</sup>O. Perković, K. Dahmen, and J. P. Sethna, *Phys. Rev. Lett.* **75**, 4528 (1995).

<sup>5</sup>P. Cizeau, S. Zapperi, G. Durin, and H. E. Stanley, *Phys. Rev. Lett.* **79**, 4669 (1997); S. Zapperi, P. Cizeau, G. Durin, and H. E. Stanley, *Phys. Rev. B* **58**, 6353 (1998).

<sup>6</sup>G. Durin and S. Zapperi, *J. Appl. Phys.* **85**, 5196 (1999).

<sup>7</sup>M. Bahiana, B. Koiller, S. L. A. de Queiroz, J. C. Denardin, and R. L. Sommer, *Phys. Rev. E* **59**, 3884 (1999).

<sup>8</sup>B. Tadić, *Physica A* **270**, 125 (1999).

<sup>9</sup>K. L. Babcock and R. M. Westervelt, *Phys. Rev. Lett.* **64**, 2168

(1990).

<sup>10</sup>P. Bak and H. Flyvbjerg, *Phys. Rev. A* **45**, 2192 (1992).

<sup>11</sup>B. Alessandro, C. Beatrice, G. Bertotti, and A. Montorsi, *J. Appl. Phys.* **68**, 2901 (1990); **68**, 2908 (1990).

<sup>12</sup>K. P. O'Brien and M. B. Weissman, *Phys. Rev. E* **50**, 3446 (1994).

<sup>13</sup>G. Bertotti, G. Durin, and A. Magni, *J. Appl. Phys.* **75**, 5490 (1994).

<sup>14</sup>N. J. Wiegman, *Appl. Phys.* **12**, 157 (1977) and other papers by the same author.

<sup>15</sup>E. Puppini and S. Ricci, *IEEE Trans. Magn.* **36**, 3090 (2000).

<sup>16</sup>D.-H. Kim, S.-B. Choe, and S.-C. Shin, *Phys. Rev. Lett.* **90**, 087203 (2003).

<sup>17</sup>A. Schwarz, M. Liebmann, U. Kaiser, R. Wiesendanger, T. W. Noh, and D. W. Kim, *Phys. Rev. Lett.* **92**, 077206 (2004).

- <sup>18</sup>A. K. Geim, S. V. Dubonos, J. G. S. Lok, I. V. Grigorieva, J. C. Maan, L. Theil Hansen, and P. E. Lindelof, *Appl. Phys. Lett.* **71**, 2379 (1997).
- <sup>19</sup>S. Pedersen, G. R. Kofod, J. C. Hollingbery, C. B. Sørensen, and P. E. Lindelof, *Phys. Rev. B* **64**, 104522 (2001).
- <sup>20</sup>D. Schuh, J. Biberger, A. Bauer, W. Breuer, and D. Weiss, *IEEE Trans. Magn.* **37**, 2091 (2001).
- <sup>21</sup>M. Rahm, J. Bentner, J. Biberger, M. Schneider, J. Zweck, D. Schuh, and D. Weiss, *IEEE Trans. Magn.* **37**, 2085 (2001).
- <sup>22</sup>Y.-C. Hsieh, S. N. Gadetsky, M. Mansuripur, and M. Takahashi, *J. Appl. Phys.* **79**, 5700 (1996).
- <sup>23</sup>J. G. S. Lok, A. K. Geim, U. Wyder, J. C. Maan, and S. V. Dubonos, *J. Magn. Magn. Mater.* **204**, 159 (1999).
- <sup>24</sup>K. S. Novoselov, A. K. Geim, D. van der Bergen, S. V. Dubonos, and J. C. Maan, *IEEE Trans. Magn.* **38**, 2583 (2002).
- <sup>25</sup>M. A. Damento and L. J. Demer, *IEEE Trans. Magn.* **23**, 1877 (1987).
- <sup>26</sup>K. S. Novoselov, S. V. Morozov, S. V. Dubonos, M. Missous, A. O. Volkov, D. A. Christian, and A. K. Geim, *J. Appl. Phys.* **93**, 10053 (2003).
- <sup>27</sup>X. Q. Li and F. M. Peeters, *Superlattices Microstruct.* **22**, 243 (1997).
- <sup>28</sup>F. M. Peeters and X. Q. Li, *Appl. Phys. Lett.* **72**, 572 (1998).
- <sup>29</sup>H. R. Hilzinger and H. Kronmüller, *J. Magn. Magn. Mater.* **2**, 11 (1976).
- <sup>30</sup>A. A. Thiele, *J. Appl. Phys.* **41**, 1139 (1970).
- <sup>31</sup>G. Bertotti, *Hysteresis in Magnetism* (Academic, New York, 1998), Sec. 11.2.3.
- <sup>32</sup>G. Durin and S. Zapperi, e-print cond-mat/0404512, 2004.
- <sup>33</sup>K. S. Novoselov, A. K. Geim, S. V. Dubonos, E. W. Hill, and I. V. Grigorieva, *Nature* **426**, 812 (2003).
- <sup>34</sup>J. S. Urbach, R. C. Madison, and J. T. Markert, *Phys. Rev. Lett.* **75**, 4694 (1995).
- <sup>35</sup>S. Lemerle, J. Ferré, C. Chappert, V. Mathet, T. Giamarchi, and P. Le Doussal, *Phys. Rev. Lett.* **80**, 849 (1998).
- <sup>36</sup>E. Puppini and M. Zani, *J. Phys.: Condens. Matter* **16**, 1183 (2004).
- <sup>37</sup>D. Ertas and M. Kardar, *Phys. Rev. E* **49**, R2532 (1994).
- <sup>38</sup>S. L. A. de Queiroz, *Phys. Rev. E* **69**, 026126 (2004).